The Feasibility of Predicting Temperature Increase through Local SAR Estimation via Electrical Properties Tomography: A Phantom Study at 7T

Xiaotong Zhang[1], Jiaen Liu[1], Pierre-Francois Van de Moortele[2], Sebastian Schmitter[2], and Bin He[1]

[1]*Department of Biomedical Engineering, University of Minnesota, Minneapolis, MN, United States,* [2]*Center for Magnetic Resonance Research, University of Minnesota, Minneapolis, MN, United States*

PURPOSE: It has been shown that Electrical Properties (EPs) (conductivity σ, permittivity ε) of biological tissues can be derived from MR-based B1 measurement[1-4]. A strong appeal for these 'Electrical Property Tomography' (EPT) methods is to estimate real-time and subject-specific local SAR induced by RF pulsing. In order to investigate the feasibility of EPT-based SAR estimation in predicting possible local temperature change, following the proposed EPT protocols in[2,3], in this preliminary study, induced local SAR in a saline phantom has been *estimated* for a heating sequence, as compared to measured temperature changes using MRI Thermometry based on the proton chemical shift (PRF)[5].

METHODS: A single-compartment cylinder phantom (12cm radius and 20cm height), consisting of H_2O, NaCl, $Cu_3SO_45H_2O$ and Gelatin (mass ratio 100:0.27:0.1:3), was constructed with conductivity 0.56S/m, permittivity 75.7, mass density 1033kg/m^3 and heat capacity $C_{phantom}$=4.2kJ/kg/ºC. EPs measurement was conducted with Agilent 85070D dielectric probe kit and an Agilent E4991A network analyzer at 298MHz. Three mineral oil phantoms were attached to the surface of phantom, providing phase drift corrections[6]. The phantom was imaged in a 7T scanner (Siemens) equipped with an elliptical 16-channel head transceiver coil[7] after being placed in the bore overnight to achieve thermal equilibrium. 12 contiguous transverse slices was chosen for the study at a spatial resolution of 1.5×1.5×3mm^3. CP2+ like B1 shim setting was employed with stronger B1 in the periphery. Temperature measurement was performed using PRF[5]. Phase maps were acquired with 3D GRE sequence (TE=10ms, TR=15ms, acquisition time 30s with 1 average and accelerated with GRAPPA2[8]), and a square RF pulse sequence (pulse duration 2ms, TR=200ms) with all gradients turned off was used for RF-heating (total time 3min). Phase maps were obtained before, during (heating 8 times with phase measurement during each interval), and after (9 phase measurements) RF-heating. These phase images were then converted into temperature maps according to[5,6].

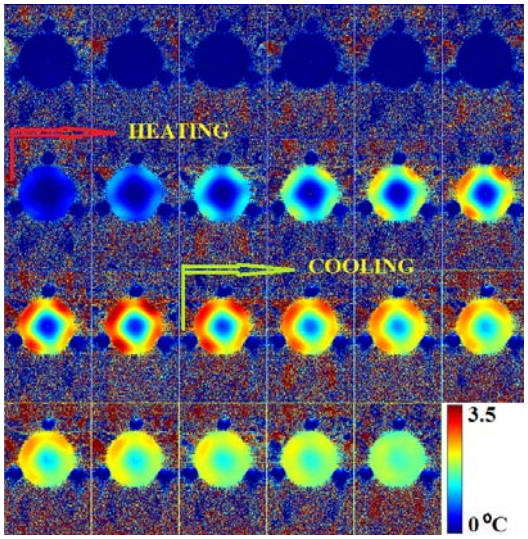

Fig.1. Temperature measurements along time using MRI Thermometry[5]. The first phase image acquired before heating was taken as the reference.

As described in[2,3], a series of 16 small flip angle GRE images were acquired with each individual channel transmitting at a time while receiving all together; a long TR, short TE, GRE image was obtained in order to produce a map of $\tilde{B}_{1,j}^{-}$ (proton density homogeneous throughout the entire phantom), after normalization by the sinus of the excitation flip angle to remove the $\tilde{B}_1^+$ component; a 3D map of the excitation flip angle was obtained with the AFI technique[9]. Based on these data, $\left|\tilde{B}_{1,k}^{+}\right|$, $\left|\tilde{B}_{1,j}^{-}\right|$ and corresponding relative phase maps were calculated[10-11]. Then utilizing measured relative phase information, the absolute phase of $\tilde{B}_{1,k}^{+}$ and $\tilde{B}_{1,j}^{-}$, and local EPs can be retrieved voxel-wisely as in[2]. Finally, the voxel-wise local SAR for the shimmed excitation can be *estimated* using complex B1 (only $\tilde{B}_1^+$ was used in this study) and reconstructed EPs under the assumption of a dominant $\left|\tilde{E}_z\right|$ compared to other electric field components as described in[3], and averaged into 10-gram SAR. For a short period time (up to several minutes) after initiation of RF-heating, effects of thermal conduction can be neglected, and the temperature increase ΔT over time τ can be treated as proportional to the induced SAR as $\Delta T=\tau SAR/C_{phantom}$[6,12]; therefore, local SAR distribution is expected to have a similar pattern with that of ΔT map.

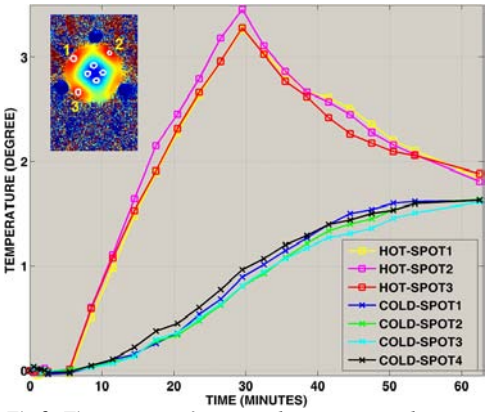

Fig.2. Time course of measured temperature change at seven local "hot" and "cold" spots.

RESULTS: ΔT maps on slice #7 measured by PRF before, during and after RF-heating are shown in Fig.1. By looking at several local spots with higher ΔT ("hot" spot, in the periphery) and lower ΔT ("cold spot", close to the center), the time course of measured temperature change has been plotted in Fig.2. In consistency with findings in [13], at hot spots where SAR is expected to be maximal and thus dominant for temperature change, prominent ΔT was observed during and after RF-heating; whereas at cold spots, SAR is expected to be minimal, and thermal conduction is dominant, thus slow but continuous temperature increase before reaching a plateau was observed once RF-heating was turned on. ΔT measurement for the 1st heating cycle (3min) – due to least thermal conduction expected during this period – was used for comparison with 10gSAR results via EPT approach.

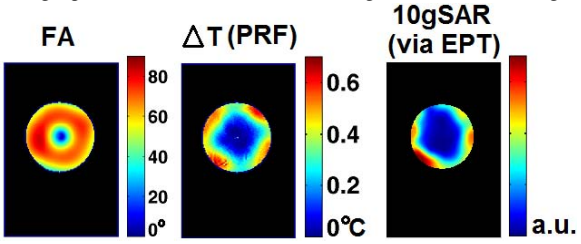

Fig.3. Measured actual flip angle (left), measured temperature change by PRF (middle), and estimated local 10gSAR (right).

On the slice of interest (slice #7), measured actual flip angle (FA) map, temperature change using PRF and estimated 10gSAR (in arbitrary unit) are shown in Fig.3. Reasonably similarity can be observed between ΔT and 10gSAR maps. The four hot spots similarly distributed in the periphery in 10gSAR map; however, their locations were "twittered" counter-clockwise compared with those in ΔT map. This is due to residual error introduced by $\tilde{B}z$ when only $\tilde{B}_1^+$ was used in reconstruction of $\left|\tilde{E}_z\right|$ [3]. This error can be eliminated by using both $\tilde{B}_1^+$ and $\tilde{B}_1^-$ to provide closed-loop estimation of $\left|\tilde{E}_z\right|$, which will be pursued in the future.

Discussion and Conclusion: Reasonable agreement has been observed between distributions of MRI Thermometry measurement and estimated SAR via EPT. Future work includes quantitative cross validation between B1 mapping-based temperature prediction and actual measured temperature (e.g. by MRI Thermometry), with the goal of further validating safety limits in the MRI scanner on a per-subject basis

References: 1) Katscher, IEEE TMI 28 :1365. 2) Zhang, MRM 69 :1285. 3) Zhang, IEEE TMI 32 :1058. 4) Sodickson, ISMRM'12 387. 5) Ishihara et al., MRM 34:814. 6) Oh, MRM DOI:10.1002/mrm.24820. 7) Adriany et al., MRM 59:590. 8) Griswold, MRM 47:1202. 9) Yarnykh, MRM 57:192. 10) Van de Moortele, MRM 54:1503. 11) Van de Moortele, ISMRM'07 1676. 12) Cloos, ISMRM'13 286. 13) Oh, MRM 63:218. **Acknowledgment:** NIH RO1EB006433, RO1EB007920, R21EB009133, R21EB014353-01A1, NSF CBET-0933067, NIH P41 RR008079, P30 NS057091, and WM KECK Foundation. We thank Dr. Xiaoping Wu for technical support.